Video Retrieval of Autonomous Driving Scenarios Based on Large Models

12310520 Rui Yuhan 12310437 Qiao Shihan

***Abstract*—Video retrieval in autonomous driving scenarios demands models to comprehend complex visual environments and align them with detailed textual descriptions. While multimodal large language models (MLLMs) have demonstrated potential in vision-language tasks, their application to domain-specific video retrieval remains underexplored. Furthermore, the scarcity of publicly available high-quality annotated video data in the autonomous driving domain makes it challenging for models to accurately learn video content semantics from limited data. Additionally, significant differences exist between autonomous driving videos and those in general video datasets, leading to suboptimal performance of generic large models on autonomous driving datasets.**

To address these challenges, we evaluate the performance of two distinct pretrained MLLMs on a carefully curated autonomous driving dataset. This dataset features high-quality captions that have undergone multi-round optimization, combining human annotation expertise with advanced automated labeling techniques, while also serving as a benchmark platform for exploring more efficient annotation strategies. Experimental results demonstrate that our approach effectively retrieves relevant video segments based on textual queries, highlighting the potential of MLLMs to enhance retrieval accuracy and scalability.

***Index Terms*—Autonomous Driving Video Retrieval, Multimodal Large Language Models (MLLMs), Video Understanding, Automated Annotation Optimization**

I. Introduction

II. Two knowledge distillation methods used

A. Research Background and Motivation of Knowledge Distillation

With the rapid advancement of large-scale foundation models, Vision-Language Models (VLMs), and Large Language Models (LLMs), deploying these models on edge devices faces significant challenges due to high computational and memory requirements. Knowledge Distillation (KD), first proposed by Hinton et al. [1], addresses this issue by training a lightweight student network under the supervision of a complex teacher model. Unlike compression methods that modify network structures, KD transfers knowledge by having the student mimic the teacher's output distribution as soft labels, enabling effective model compression while maintaining performance. Additionally, KD facilitates knowledge transfer from source tasks to target tasks with limited labeled data, making it particularly valuable for domain-specific applications such as autonomous driving video retrieval.

1) Mainstream Knowledge Distillation Approaches: Knowledge distillation methods can be categorized based on the source of knowledge being distilled [2]. The three primary categories are: **logit-based distillation**, which transfers final predictions using softmax with temperature to create soft labels; **feature-based distillation**, which transfers intermediate layer representations and attention maps, providing richer information than logits alone; and **similarity-based distillation**, which transfers structural knowledge through pairwise similarities between features, channels, or instances. Additionally, distillation can be organized by training schemes: **offline distillation** (pre-trained teacher with frozen weights), **online distillation** (simultaneous training), and **self-distillation** (same network transferring knowledge across layers or stages). Other notable approaches include **attention-based distillation**for transferring focus patterns, **contrastive distillation** leveraging contrastive learning principles, and **cross-modal distillation** for transferring knowledge between different modalities, which is particularly relevant for multimodal tasks like video retrieval.

B. DLDKD

DLDKD (Dual Learning with Dynamic Knowledge Distillation) [3] employs a dual-stream teacher-student framework that transfers knowledge from a large teacher model to a lightweight student model through multi-level distillation.

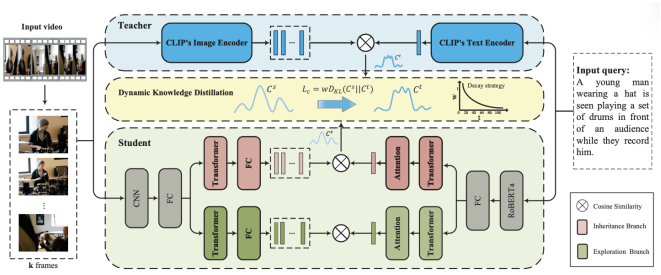

Fig. 1. The framework of DLDKD.

DLDKD performs distillation at multiple levels: feature-level distillation transfers intermediate representations, logit-level distillation aligns output distributions, and attention-level distillation preserves attention patterns.

1) Loss Functions: The DLDKD framework employs a dual learning objective that combines knowledge from the teacher model with task-specific learning through two student branches. The total loss function is defined as:

$$\mathcal{L}_{total} = \lambda_I \mathcal{L}_I + \lambda_E \mathcal{L}_E + \mathcal{L}_{task} \tag{1}$$

where λ_I and λ_E are dynamic weights that adjust the contribution of the inheritance branch and exploration branch losses, respectively.

Inheritance Student Branch Loss ($\mathcal{L}_I$): The inheritance branch learns to absorb knowledge from the teacher model

through multi-level distillation. The loss combines feature-level, logit-level, and attention-level distillation:

$$\mathcal{L}_I = \alpha_f \mathcal{L}_{feat} + \alpha_l \mathcal{L}_{logit} + \alpha_a \mathcal{L}_{attn} \tag{2}$$

where α_f, α_l, and α_a are weights for feature-level, logit-level, and attention-level distillation losses, respectively.

The feature-level distillation loss aligns intermediate representations between teacher and student:

$$\mathcal{L}_{feat} = \frac{1}{N} \sum_{i=1}^{N} \|F_t^{(i)} - F_s^{(i)}\|_2^2 \tag{3}$$

where $F_t^{(i)}$ and $F_s^{(i)}$ denote the feature representations at layer i from the teacher and student models, respectively, and N is the number of layers used for feature distillation.

The logit-level distillation loss uses KL divergence to align output distributions:

$$\mathcal{L}_{logit} = \text{KL}(\text{softmax}(z_t/\tau) \| \text{softmax}(z_s/\tau)) \tag{4}$$

where z_t and z_s are the logits from teacher and student models, and τ is the temperature parameter for softening the distributions.

The attention-level distillation loss preserves the teacher's attention patterns:

$$\mathcal{L}_{attn} = \frac{1}{L} \sum_{l=1}^{L} \|A_t^{(l)} - A_s^{(l)}\|_F^2 \tag{5}$$

where $A_t^{(l)}$ and $A_s^{(l)}$ are attention maps at layer l from teacher and student models, L is the number of attention layers, and $\|\cdot\|_F$ denotes the Frobenius norm.

Exploration Student Branch Loss ($\mathcal{L}_E$): The exploration branch focuses on task-specific learning to capture domain-specific patterns that may not be fully represented in the teacher model:

$$\mathcal{L}_E = -\frac{1}{B} \sum_{i=1}^{B} \log \frac{\exp(\text{sim}(v_i, t_i^+)/\tau_E)}{\sum_{j=1}^{B} \exp(\text{sim}(v_i, t_j)/\tau_E)} \tag{6}$$

where B is the batch size, v_i is the video embedding, t_i^+ is the positive text query, $\text{sim}(\cdot,\cdot)$ computes cosine similarity, and τ_E is the temperature parameter for the exploration branch.

Task-Specific Loss ($\mathcal{L}_{task}$): The task loss ensures that the final model performs well on the video-text retrieval task:

$$\mathcal{L}_{task} = \mathcal{L}_{retrieval} = -\log P(v^+|t) - \log P(t^+|v) \tag{7}$$

where $P(v^+|t)$ and $P(t^+|v)$ represent the probabilities of retrieving the correct video given text query and vice versa.

Dynamic Weight Adjustment: The weights λ_I and λ_E are dynamically adjusted during training based on the performance of each branch. This allows the framework to automatically balance between teacher knowledge inheritance and task-specific exploration:

$$\lambda_I^{(t)} = \lambda_I^{(0)} \cdot \exp(-\gamma_I \cdot t), \quad \lambda_E^{(t)} = \lambda_E^{(0)} \cdot (1 + \gamma_E \cdot t) \tag{8}$$

where t is the training epoch, $\lambda_I^{(0)}$ and $\lambda_E^{(0)}$ are initial weights, and γ_I, γ_E are decay/growth rates that control the dynamic adjustment schedule.

2) Feature Pre-Extraction Strategy: DLDKD employs feature pre-extraction to accelerate training: teacher model features are pre-computed and cached for all training samples before distillation training, eliminating repeated forward passes through the teacher model during training. In the subsequent modifications to TeachCLIP, we will incorporate this feature pre-extraction strategy to shorten the training time.

C. TeachCLIP

1) Inspiration: Existing VTR models generally fall into two categories: lightweight global feature models (e.g., CLIP4Clip) and heavy fine-grained models (e.g., X-CLIP). The former is computationally efficient but often lacks frame-level details, resulting in suboptimal retrieval accuracy. The latter leverages frame-level interactions to enhance performance but incurs high computational costs.

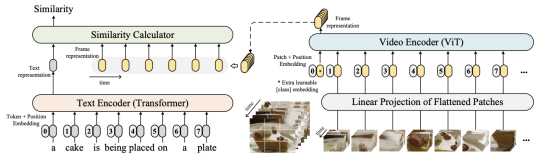

(a) CLIP4Clip Framework

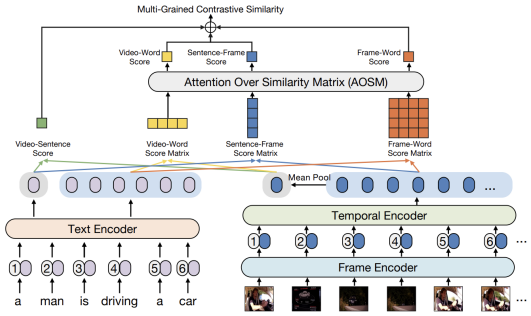

(b) X-CLIP Framework

Fig. 2. Comparison of CLIP4Clip and X-CLIP frameworks. Both use similar bottom-up encoding but differ in upper-layer feature usage.

In terms of vision and text encoding, both CLIP4Clip and X-CLIP share nearly identical bottom-level encoding mechanisms (Frame $\rightarrow$ Patch $\rightarrow$ ViT, Word $\rightarrow$ Embedding $\rightarrow$ Transformer). The primary distinction lies in how they utilize these features in the upper layers: CLIP4Clip performs pooling to retain only global video vectors, whereas X-CLIP preserves fine-grained features and performs multi-granularity alignment.

TeachCLIP aims to bridge this gap by distilling the fine-grained alignment capability of heavy models into a lightweight student model.

2) Framework: The TeachCLIP framework is designed to transfer the fine-grained knowledge from a teacher model to a student model while maintaining high inference efficiency.

Student Model: The student model is built upon CLIP4Clip. It samples the video into frames, processes each frame through the CLIP ViT to obtain frame features, and enhances them via a temporal Transformer. A key innovation

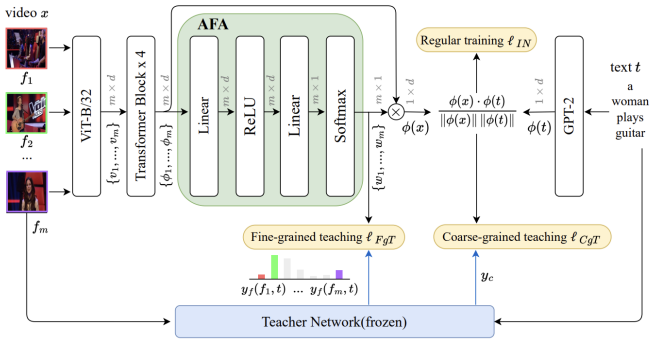

Fig. 3. The framework of TeachCLIP.

is replacing the original mean pooling with Attentional Frame-Feature Aggregation (AFA). AFA generates frame weights $\{w_i\}$ to compute a weighted sum of frame features:

$$\phi(x) = \sum_{i=1}^{m} w_i \cdot \phi_i \tag{9}$$

The AFA module consists of a lightweight structure (Linear $\rightarrow$ ReLU $\rightarrow$ Linear $\rightarrow$ Softmax) and introduces negligible parameters.

Teacher Model: The teacher model provides two types of supervision:

- **Video-level soft labels (y_c):** The teacher provides the distribution of video-text correlations to guide the student's ranking.
- **Frame-level soft labels (y_f):** The teacher provides the distribution of frame-text correlations to guide the student's frame weight allocation in AFA.

Learning Objectives: The training involves three losses:

1) *Frame-level Distillation (ℓ_{FgT}):* Optimizes the AFA weights to match the teacher's frame-text similarity distribution. The loss function is defined as:

$$\ell_{FgT} = -\frac{1}{b} \sum_{i=1}^{b} \sum_{k=1}^{m} y_f(f_{i,k}, t_i) \log w_{i,k} \tag{10}$$

where b is the batch size, m is the number of frames, and y_f represents the frame-text similarity from the teacher.

2) *Video-level Distillation (ℓ_{CgT}):* Aligns the student's video-text similarity matrix with the teacher's multi-grained similarity matrix using the Pearson distance d_p:

$$\begin{aligned} \ell_{CgT} = &\frac{1}{b} \sum_{i} d_p(\sigma(B_{i,\cdot}), \sigma(y_c(v_i, \cdot))) \\ &+ \frac{1}{b} \sum_{j} d_p(\sigma(B_{\cdot,j}), \sigma(y_c(\cdot, t_j))) \end{aligned} \tag{11}$$

where σ denotes the softmax function and B is the similarity matrix of the student.

3) *Contrastive Learning (ℓ_{IN}):* Standard maximization of similarity for positive pairs and minimization for negative pairs, using symmetric InfoNCE loss:

$$\ell_{IN} = \frac{1}{2} \left[\ell_{NCE}^{v \rightarrow t} + \ell_{NCE}^{t \rightarrow v} \right] \tag{12}$$

where

$$\ell_{NCE}^{v \rightarrow t} = -\frac{1}{b} \sum_{i=1}^{b} \log \frac{\exp(B_{ii}/\tau)}{\sum_{j=1}^{b} \exp(B_{ij}/\tau)} \tag{13}$$

and $\ell_{NCE}^{t \rightarrow v}$ is defined symmetrically.

The total loss is $\ell = \ell_{CgT} + \ell_{FgT} + \ell_{IN}$. During inference, the teacher model is discarded, and only the lightweight student model with AFA is used.

3) TeachCLIP vs X-CLIP Parameters and FLOPs Comparison: Table I presents the comparison of parameters and FLOPs between TeachCLIP and the teacher model (X-CLIP).

TABLE I
COMPARISON OF PARAMETERS AND FLOPS

Model	Parameters	FLOPs (Inference)	Description
TeachCLIP	$\approx$ 200M	53.65G (12 frames)	Student model, based on CLIP4Clip + AFA, maintains lightweight inference
X-CLIP (Teacher)	$\approx$ 220M	145G (8 frames) / 287G (16 frames)	Teacher model, introduces multi-grained contrastive similarity, higher inference cost

III. ALTERATIONS ON TEACHCLIP

A. On Student Model

We explored replacing the Transformer-based visual encoder (ViT) in the student model with a Convolutional Neural Network (CNN) architecture, specifically ConvNeXt, leveraging the pre-trained weights from OpenCLIP [**?**]. The motivation behind this substitution lies in the inherent inductive biases of CNNs, such as translation invariance and locality, which can be advantageous for visual feature extraction. Additionally, lightweight CNN variants offer potential improvements in inference efficiency and reduced memory footprint compared to heavy ViT-based models.

1) Exploration under OpenCLIP Framework on COCO Dataset: To validate the feasibility of ConvNeXt as a visual encoder and identify effective fine-tuning strategies, we first conducted a series of experiments on the relatively smaller COCO dataset using ConvNeXtV2-Tiny. We compared three main strategies: full fine-tuning (No Freeze), gradual unfreezing (Unfreeze 3-5), and replacing the text tower. The results, summarized in Table II, indicate that full fine-tuning leads to overfitting due to the large parameter space relative to the data size. Conversely, a strategy of "controlled trainable subsets with gradual unfreezing"—specifically, unfreezing the text tower at epoch 3 and the visual tower at epoch 5—yielded the best performance (I2T R@1: 9.55%), serving as a constrained fine-tuning approach that balances plasticity and stability.

Building on the Tiny experiments, we further optimized the approach using a larger model, ConvNeXt-Base with an attentional pooling layer ('absattn'), exploring four iterative strategies. As shown in Table III, we started with a baseline using a three-stage unfreezing schedule. Introducing knowledge distillation from a teacher model while keeping the student

TABLE II
COMPARISON OF CONVNEXTV2-TINY STRATEGIES ON COCO

Strategy	I2T R@1	Observation
No Freeze (Full Fine-tuning)	8.12%	Overfitting, worst performance
Unfreeze 3-5 (Gradual)	**9.55%**	**Best balance, effective constraint**
Change Text Tower + Unfreeze	9.07%	Intermediate performance

frozen significantly improved performance by providing strong regularization. However, attempting to unfreeze the backbone in later stages under distillation degraded performance, suggesting that the added freedom undermined the distillation constraints. The most effective strategy proved to be removing distillation but introducing a Head-level Alignment loss ('headalign') combined with earlier, small-scale unfreezing. This approach achieved the highest R@1 of 13.11%, demonstrating that a well-designed alignment loss with precise unfreezing rhythms can outperform simple distillation.

TABLE III
ITERATIVE OPTIMIZATION OF CONVNEXT-BASE ON COCO

Strategy	I2T R@1	Note
Baseline (3-stage Unfreeze)	12.34%	Standard gradual unfreezing
Distill + Frozen	13.10%	Strong regularization via teacher
Distill + Late Unfreeze	12.98%	Unfreezing hurts distillation constraint
Head Align + Early Unfreeze	**13.11%**	**Best strategy, replaces distillation**

2) Preliminary Implementation on TeachCLIP with MSRVTT Dataset: Applying these insights to the video retrieval task, we integrated the ConvNeXt-Base encoder initialized from OpenCLIP into the TeachCLIP student framework. We tested the direct migration of the architecture on the MSRVTT dataset. However, as shown in Table IV, the preliminary results were suboptimal compared to the image-text experiments. Even with a strategy that locked the encoder and only trained the alignment heads, the performance remained limited (Text-to-Video R@1 $\approx$ 2.6–3.4%). This suggests that a direct replacement of the student encoder without specialized adaptation for video temporal dynamics—such as the 'absattn' or more complex temporal aggregation modules validated in the OpenCLIP experiments—is insufficient. Future work is needed to better adapt the convolutional features for temporal coherence in video tasks.

TABLE IV
PRELIMINARY RESULTS OF CONVNEXT-BASED STUDENT ON MSRVTT

Setting	Text-to-Video R@1
MSRVTT-9k (10 epochs)	3.4%
MSRVTT-7k (10 epochs)	2.5%
MSRVTT-7k (16 epochs, Locked Encoder)	2.6%

B. On teacher model

IV. POST-TRAINING QUANTIZATION OF VAST MODEL USING MS-SWIFT

In this section, we apply post-training quantization methods introduced in MS-Swift [4] to compress the VAST model [5] for video-text retrieval tasks. Post-training quantization is a model compression technique that reduces the precision of model weights and activations after the model has been fully trained, enabling efficient deployment on resource-constrained devices without requiring retraining from scratch.

A. MS-Swift Quantization Architecture and Methodology

MS-Swift (ModelScope Swift) [4] implements a GPTQ-based quantization framework for post-training quantization. The framework employs GPTQ with INT4 precision, using block-wise sequential quantization with Hessian-based optimization to minimize reconstruction error. Key configuration parameters include: group size of 128 for grouped quantization, symmetric quantization (sym=true), and sequential quantization (true_sequential=true) to preserve inter-layer dependencies. The framework supports module-level selective quantization, enabling quantization to be applied only to specific components (e.g., vision encoder blocks) while preserving full precision for other modules such as text encoders or modality-specific branches in multimodal models.

B. VAST Architecture for Video-Text Retrieval

VAST (Vision-Audio-Subtitle-Text) [5] is an omni-modality foundation model. The VAST framework architecture is illustrated in Figure 4.

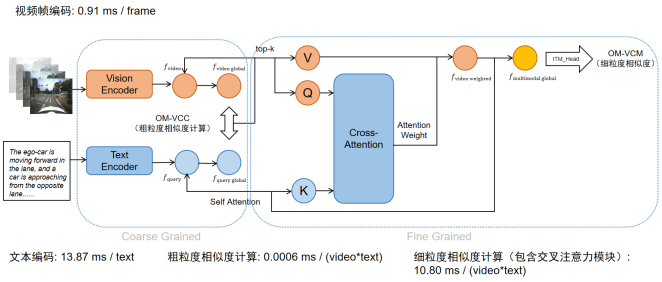

Fig. 4. The framework of VAST.

For video-text retrieval, VAST employs dual encoders: a video encoder that processes frames through a ViT architecture with temporal modeling, and a text encoder based on transformer architecture. The model learns cross-modal alignment in a shared embedding space, using contrastive learning to maximize similarity between matching video-text pairs.

The VAST model achieves strong performance in video-text retrieval after fine-tuning on domain-specific data. Given the model's size, there is room for further lightweight optimization to better adapt to real-time applications. We therefore apply post-training quantization to obtain smaller model weights while maintaining competitive performance.

C. Post-Training Quantization Experimental Process

We apply GPTQ-based post-training quantization to compress the fine-tuned VAST model from FP16 to INT4 precision, achieving approximately 4× model size reduction while preserving retrieval performance.

Quantization Setup: The quantization is performed on the fine-tuned VAST model using MS-Swift's GPTQ implementation. We configure the quantization to target INT4 precision with the following key parameters: group size of 128 for grouped quantization, symmetric quantization (sym=true), and sequential quantization (`true_sequential`=true) to maintain layer dependencies. The quantization is selectively applied only to the vision encoder blocks (`vision_encoder.visual.blocks`), preserving the full precision of other components including the text encoder and audio branches.

Calibration Data: We use 200 calibration samples in JSONL format, each containing text queries and corresponding image frame sequences. During quantization, these samples are forward-passed through the model to collect activation statistics for each layer. The collected activations are used to compute Hessian matrices, which guide the quantization parameter optimization to minimize reconstruction error.

Quantization Process: The quantization proceeds block-by-block through 40 vision encoder blocks. For each block, four linear modules are quantized sequentially: attention QKV projection (`attn.qkv`), attention output projection (`attn.proj`), and MLP layers (`mlp.fc1`, `mlp.fc2`). The process involves collecting activations from calibration data, computing Hessian matrices for weight sensitivity, performing grouped quantization (group size 128) to convert FP16 weights to INT4, and applying error compensation. Weights are transformed from FP16 (16 bits) to INT4 (4 bits) with per-group scaling factors, achieving approximately 4× compression with 4 INT4 values packed into 1 INT16 for storage.

The quantized VAST model maintains competitive retrieval performance with significantly reduced model size and memory footprint, enabling more efficient deployment for real-time video-text retrieval applications.

D. Quantization Results and Comparison

Table V presents a comprehensive comparison between the original FP16 model and the quantized INT4 model, demonstrating the effectiveness of the GPTQ-based quantization approach.

TABLE V
COMPARISON OF MODEL STATISTICS BEFORE AND AFTER QUANTIZATION

Metric	FP16	INT4	Ratio
File Size	5.20 GB	1.86 GB	2.80×
Total Parameters	1,396.66M	522.85M	2.67×
Vision Encoder	1,136.44M	262.62M	4.33×
Total Weight Size	5.33 GB	1.99 GB	2.67×

The quantization results demonstrate effective compression: the vision encoder achieved 4.33× compression, closely matching the theoretical 4× ratio for INT4 quantization. The overall model size was reduced from 5.20 GB to 1.86 GB (2.80×), while the total compression ratio (2.67×) is lower due to other components remaining at full FP32 precision as part of the selective quantization strategy.

Table VI presents the retrieval performance comparison on the suscape test set (autonomous driving scenario dataset) before and after quantization.

TABLE VI
RETRIEVAL PERFORMANCE COMPARISON ON SUSCAPE TEST SET

Metric	FP16	INT4
Recall@1	64.4	37.3
Recall@5	88.7	55.9
Recall@10	97.2	65.2
Average Recall	83.4	52.8

The quantized model shows expected performance degradation compared to the full-precision model. Despite the performance drop, the quantized model maintains reasonable retrieval capabilities while achieving significant model size reduction.

V. CONCLUSION

Autonomous driving video retrieval presents unique challenges due to the complexity of real-world driving scenarios and the scarcity of high-quality annotated datasets. In this work, we explored the potential of multimodal large language models (MLLMs) to bridge the gap between visual perception and textual understanding in autonomous driving contexts. By leveraging a carefully curated dataset with optimized annotations, combining human expertise and automated refinement using Video-LLama2, we demonstrated that pretrained MLLMs can be effectively adapted for domain-specific video retrieval tasks.

Our experiments with two state-of-the-art MLLMs (Vast and Clip-Vip) revealed that fine-tuning on high-quality annotated data significantly improves retrieval accuracy, validating the importance of robust dataset construction. Additionally, our work establishes a benchmark for future research in autonomous driving video understanding, providing a foundation for developing more interpretable and scalable retrieval systems.

Moving forward, we anticipate that further advancements in MLLMs, combined with more sophisticated annotation pipelines, will enhance the generalization capabilities of autonomous driving systems. Future research could explore dynamic annotation strategies, real-time retrieval optimization, and the integration of multi-sensor data (e.g., LiDAR and radar) to further improve model performance in complex driving environments.

Ultimately, this study highlights the critical role of high-quality data and domain-specific adaptation in advancing autonomous driving technologies, paving the way for safer and more intelligent transportation systems.

REFERENCES

[1] G. Hinton, O. Vinyals, and J. Dean, "Distilling the knowledge in a neural network," *arXiv preprint arXiv:1503.02531*, 2015, nIPS 2014 Deep Learning Workshop. [Online]. Available: https://arxiv.org/abs/1503.02531

[2] A. M. Mansourian, R. Ahmadi, M. Ghafouri, A. M. Babaei, E. B. Golezani, Z. Y. Ghamchi, V. Ramezanian, A. Taherian, K. Dinashi, A. Miri, and S. Kasaei, "A comprehensive survey on knowledge distillation," *Transactions on Machine Learning Research*, 2025, published at TMLR, arXiv:2503.12067. [Online]. Available: https://arxiv.org/abs/2503.12067

[3] J. Dong, M. Zhang, Z. Zhang, X. Chen, D. Liu, X. Qu, X. Wang, and B. Liu, "Dual learning with dynamic knowledge distillation for partially relevant video retrieval," in *Proceedings of the IEEE/CVF International Conference on Computer Vision (ICCV)*, 2023, pp. 11 302–11 312.

[4] Y. Zhao, J. Huang, J. Hu, X. Wang, Y. Mao, D. Zhang, H. Zhang, Z. Jiang, Z. Wu, B. Ai, A. Wang, W. Zhou, and Y. Chen, "Swift: A scalable lightweight infrastructure for fine-tuning," 2024. [Online]. Available: https://arxiv.org/abs/2408.05517

[5] S. Chen, H. Li, Q. Wang, Z. Zhao, M. Sun, X. Zhu, and J. Liu, "Vast: A vision-audio-subtitle-text omni-modality foundation model and dataset," *Advances in Neural Information Processing Systems*, vol. 36, 2023, neurIPS 2023. [Online]. Available: https://arxiv.org/abs/2305.18500